

NASA Technical Memorandum 86332

NASA-TM-86332 19850006570

FATIGUE BEHAVIOR OF CONTINUOUS FIBER
SILICON-CARBIDE/ALUMINUM COMPOSITES

W. S. JOHNSON AND R. R. WALLIS

DECEMBER 1984

LIBRARY COPY

JAN 8 1985

LANGLEY RESEARCH CENTER
LIBRARY, NASA
HAMPTON, VIRGINIA



National Aeronautics and
Space Administration

Langley Research Center
Hampton, Virginia 23665



SUMMARY

Four lay-ups of continuous fiber silicon carbide (SCS_2) fiber/aluminum matrix composites were tested to assess fatigue mechanisms including stiffness loss when cycled below their respective fatigue limits. The lay-ups were $[0]_8$, $[0_2/\pm 45]_s$, $[0/90]_{2s}$, and $[0/\pm 45/90]_s$. The data were compared with predictions from the first author's previously published shakedown model which predicts fatigue-induced stiffness loss in metal matrix composites. A fifth lay-up, $[\pm 45]_{2s}$, was tested to compare the shakedown and fatigue limits. The particular batch of silicon-carbide fibers tested in this program had a somewhat lower modulus (340 GPa) than expected and displayed poor bonding to the aluminum matrix. Good agreement was obtained between the stiffness loss model and the test data. The fatigue damage below the fatigue limit was primarily in the form of matrix cracking. The fatigue limit corresponded to the laminate shakedown limit for the $[\pm 45]_{2s}$ laminate.

N85-14879 #

NOMENCLATURE

E^f	Fiber elastic modulus, MPa
E^m	Matrix elastic modulus, MPa
E_{eff}^m	Effective modulus of the matrix in the loading direction, MPa
E_0	Initial elastic modulus of the first cycle (modulus of undamaged laminate), MPa
E_s	Secant modulus, MPa
E_{SDS}	Laminate modulus assuming damaged matrix material, MPa
R	Stress ratio, S_{\min}/S_{\max}
S_{\max}	Maximum laminate stress, MPa
S_{\min}	Minimum laminate stress, MPa
Y	Maximum cyclic yield stress, MPa
$\Delta\epsilon$	Laminate strain range
$\Delta\epsilon_{\text{comp}}^m$	Compressive strain range of the matrix material in the loading direction
ΔS	Laminate stress range, MPa
ΔS_{sh}	Maximum laminate stress range that causes no fatigue damage (shakedown stress range), MPa
σ^f	Axial stress in the fiber in the loading direction, MPa
σ^m	Axial stress in the matrix in the loading direction, MPa
σ_{sh}^m	Stress in the matrix material in the loading direction at the laminate shakedown limit, MPa

INTRODUCTION

Metal matrix composites (MMC) are currently being considered for use on missiles, aircraft and other high performance vehicles where low weight and high stiffness are important. Continuous fiber MMC exhibit high directional stiffness and strength-to-weight ratios. However these composites are expensive. A commercially available continuous silicon-carbide fiber, designated SCS₂, has been developed by AVCO Specialty Materials Division of Lowell, Mass., and is expected to be much more economical to produce than the most commonly used continuous fibers for MMC, boron. Therefore, silicon carbide/aluminum composites are expected to be more cost competitive with metals and epoxy resin composites. The purpose of this paper is to examine the stiffness loss behavior of five lay-ups of SCS₂/Al composites and assess the applicability of the stiffness loss model proposed in reference [1].

Previous research on the fatigue behavior of boron/aluminum composites [1-5] has shown that boron/aluminum can develop significant internal matrix cracking even when cycled below the fatigue limit. This results in laminate modulus loss. In quasi-isotropic laminates, matrix cracks reduce stiffness as much as 40 percent. Because most MMC structural components are expected to be stiffness critical, even a small drop in component stiffness may render the part useless or cause failure of the structure. Therefore this paper focuses on the stiffness loss in the SCS₂/Al composites as a function of cyclic loading and not on final laminate failure. Only the [±45]_{2s} laminate will be examined by establishing the fatigue limit and comparing it with the calculated shakedown limit.

EXPERIMENTAL PROCEDURE

Composite Laminate

The material tested was unnotched silicon carbide composite with a 6061 aluminum matrix and 0.14-mm diameter SCS_2 fibers provided by the manufacturer. Table I presents material properties for the SCS_2 and aluminum constituents. The specimens were straight-sided with a width of 19.0 mm and a thickness of 1.6 mm. Each laminate had a fiber volume fraction of 0.44. All the specimens were annealed before testing. All the specimens were fatigue loaded at 10 cycles per second except when the stress-strain response of the material was recorded on an X-Y plotter. The stress-strain data were taken under quasi-static conditions at 1, 2, 3, 4, 5, 10, 50, 100, 500, 1,000, 5,000, 50,000, 100,000, and 500,000 cycles for each stress level. The strain was measured with a 25.4-mm gage length extensometer. Except for the $[\pm 45]_{2s}$ laminates, all the specimens were cycled at constant amplitude stress levels below stress levels which would cause failure in 500,000 cycles. The stress ratio, R , was constant for each test. All tests were conducted at $R = 0.1$ except for a few specimens of $[0_2/\pm 45]_s$ which were also tested at a $R = 0.3$.

In the present study, the tests were conducted at a constant cyclic stress range for 500,000 cycles (time enough for a saturation damage state to develop), and then the stress-strain response was recorded. The stress range was then increased to a new desired level, and another 500,000 cycles applied. The resulting stress-strain response was recorded. This process was repeated up to as many as five different stress levels per specimen. Saturation fatigue damage at each level depends only on the applied stress range and, therefore, is not influenced by the prior cycling at lower stress ranges as shown in reference [2]. This test method was also used with success to generate data in reference [1]. The $[\pm 45]_{2s}$ laminates were cycled to failure

or 2 million cycles (whichever occurred first) to determine their fatigue limit.

Fibers

Individual SCS₂ fibers were pulled in tension to determine their elastic modulus. The fibers were obtained by leaching away the aluminum matrix of a [0/90]_{2s} and [0]₈ laminate using a hydrochloric acid solution. Since the fiber cross section is round, the diameters were easily measured with a micrometer in order to calculate cross-sectional area. The individual fibers were bonded and aligned between thin aluminum tabs to facilitate gripping. Three fiber lengths were tested: 51 mm, 76 mm, and 102 mm.

The specimens were then loaded in a table-top screw driven machine where the crosshead displacement and load were recorded. The elastic modulus of the fiber was calculated from the load-displacement curve.

ANALYSIS

If fatigue damage in general is to be avoided, the cyclic loading must produce only elastic strains in the constituents. Even so, local plastic straining can be permitted in the composite during the first few load cycles, provided that the composite "shakes down" during these few cycles. The shakedown state is reached if the matrix cyclically hardens to a cyclic yield stress, Y , such that, subsequently, only elastic deformation occurs under load cycles. The shakedown limit for the composite containing 0° fibers is considerably below the composite's fatigue limit [4]. Previous tests have shown that the matrix fatigue limit coincides with the maximum stable cyclic yield stress for annealed aluminum [4,6] and steels [6]. The value of Y is 70 MPa for the annealed 6061 aluminum [4].

The shakedown stress range for a unidirectionally loaded laminate can be found by using laminate theory to determine the yield surfaces for individual

plies in the laminate. For the experimental program reported herein, the shakedown stress range, ΔS_{sh} , is the width of the overall yield surface in the direction of the applied uniaxial loading. The value of ΔS_{sh} can be calculated easily with the computer program AGLPLY [7]. The AGLPLY program incorporates a modified materials model, and not a straight series model, to determine lamina transverse properties. Input for the AGLPLY program consists of the following: the fiber elastic modulus and Poisson's ratio; the matrix's elastic modulus, Poisson's ratio, and cyclic yield stress; the fiber volume fraction of each ply; the fiber angle orientation of each ply; and the relative thickness of each ply. The laminate stress that causes first yielding in the matrix of any ply is printed out. This laminate stress is half of the shakedown stress range. More details on this procedure can be found in references [3] [4] and [7].

The shakedown stress range is used in conjunction with the stiffness loss model [1] to develop a cyclic strain versus cyclic stress relationship for a given laminate. As shown in Figure 1, when the cyclic stress range ΔS exceeds the shakedown range, ΔS_{sh} , the matrix is assumed to respond as an elastic-perfectly plastic material along the dotted line for the first few cycles. The matrix stress cycles between $+\sigma_{sh}^m$ and $-\sigma_{sh}^m$ where σ_{sh}^m equals half the shakedown strain range times the undamaged matrix modulus E^m . That is

$$\sigma_{sh}^m = (\Delta S_{sh}/2E_0)E^m$$

With continued load cycling, cracks form in the matrix. The cracks open on tensile excursions and close on compressive excursions of the matrix stress, leading to the behavior represented by the solid line in Figure 1.

For a given total strain range $\Delta\epsilon$, as shown in Figure 2, the effective tensile modulus of the matrix E_{eff}^m can be written

$$E_{\text{eff}}^m = \sigma_{\text{sh}}^m / (\Delta\epsilon - \Delta\epsilon_{\text{comp}}^m)$$

where

$$\Delta\epsilon_{\text{comp}}^m = \Delta S_{\text{sh}} / 2E_0$$

which is the compressive strain range of the matrix. This modulus is entered into a laminate analysis to obtain the laminate tensile modulus, E_{SDS} , which is then used to estimate the secant modulus for the damaged laminate. The laminate stress-strain relation is stated as

$$\Delta S = \left(\Delta\epsilon_{\text{comp}}^m \right) E_0 + \left(\Delta\epsilon - \Delta\epsilon_{\text{comp}}^m \right) E_{\text{SDS}}$$

from which ΔS is calculated for strain-controlled tests. The laminate secant modulus prediction is then

$$E_S = \Delta S / \Delta\epsilon$$

RESULTS AND DISCUSSION

Fiber Modulus

Initial laminate elastic moduli measurements were considerably less than predicted by laminate analysis. Since the predictions were excellent in an earlier study on boron/aluminum [4], this large discrepancy needed to be resolved. The original moduli predictions were made using a fiber modulus of

390 GPa as suggested by the manufacturer. Since the aluminum modulus is 72.5 GPa and the fiber volume fraction is easily measured, the fiber modulus is the only uncertain parameter.

Individual fibers were tested to determine the modulus used in the current work. Table II lists the fiber moduli for the two laminates and three fiber lengths. The $[0/90]_{2s}$ fibers show average moduli slightly lower than the $[0]_8$ fibers. Further, the 51-mm fiber gage length showed a lower average modulus than the 76- and 102-mm gage length. This indicated some sensitivity to gage length tested probably due to slippage of the fibers. The results of the 76- and 102-mm gage lengths were very close to each other. A modulus value of 340 GPa was chosen to represent the fiber. According to reference [8], production process problems (carbon rich deposition zones) that were occurring when these fibers were produced may have resulted in lower than normal fiber strength and modulus. The production process problems have been resolved since then and fiber moduli of approximately 400 GPa are being achieved routinely [9].

Laminate Properties

The shakedown stress range, ΔS_{sh} , and E_o were calculated using the fiber modulus of 340 GPa as shown in Table III. Figure 3 shows the predicted initial elastic modulus using 340 GPa versus the experimental. The predictions are quite good with the largest error of 15 percent for the $[\pm 45]_{2s}$ laminate. This can be due to even lower fiber moduli than the 340 GPa measured or due to bad fiber matrix interface as will be discussed next.

Fiber Matrix Interface

The fiber matrix interface was noticeably weaker for these SCS_2/Al composites than for the previously tested B/Al . This was evident by more fiber pull-out during static strength tests of the SCS_2/Al laminates than

previously observed for B/Al laminates and by the separation of the matrix and fiber during fatigue tests of the $[0_2/\pm 45]_S$ lay-up. Figure 4 shows a micrograph of early fiber/matrix separation. After continued cycling at a higher stress level, these separations join together to form an edge delamination as shown in Figures 4 and 5. Figure 6 shows the extent of the edge delamination into the specimen. The $[0_2/\pm 45]_S$ lay-up was the only laminate tested that showed the edge delamination as described, indicating that this plate must have had poorer quality bonding between the fiber and matrix than the others tested. If this edge delamination was due to high interlaminar stresses (as common in graphite/epoxy composites), it would be expected that delamination would have occurred in the $[0/\pm 45/90]_S$ laminate since that lay-up has the highest interlaminar stresses of those tested.

Stiffness Loss and Predictions

The predicted cyclic stress-strain response after 500,000 cycles and its associated secant modulus are presented in this section and compared with measured experimental results. The predictions are shown as solid lines (see Fig. 7 as an example). For reference, the dashed line is the undamaged elastic modulus of the laminate. The secant modulus scale can be read in two ways. First, entering on the ΔS axis, crossing to the solid prediction line and down to the secant modulus scale gives the predicted secant modulus of a laminate after 500,000 cycles at a given stress range. Second, one could simply rise from the cyclic strain scale directly to the secant modulus scale to assess the secant modulus after 500,000 cycles of a given strain range. As shown in reference [1], the same saturation damage state will be reached whether the test is a constant stress or a constant strain controlled test. Notice that the secant modulus scale is nonlinear. Also notice that the

secant modulus scale ends on the left at the shakedown limit; the secant modulus is equal to E_0 below the shakedown limit.

Figure 7 presents the data and predictions for the $[0]_8$ laminate. The predictions are quite good. Approximately 10 percent of the secant modulus was lost after 500,000 cycles at a cyclic strain range of 0.004.

The $[0_2/\pm 45]_S$ data are shown in Figure 8. Both the $R = 0.1$ and 0.3 data behave the same, indicating once again [2,4] that the matrix damage described herein is a function of stress range and not mean stress. There is very good agreement between predictions and data. The previously discussed delamination apparently does not decrease the stiffness beyond that due to the predicted matrix cracking. The $[0_2/\pm 45]_S$ laminate had a 30 percent loss in secant modulus at $\Delta\epsilon = 0.004$.

The $[0/90]_2S$ predictions as shown in Figure 9 were not very good compared to the other laminates. Approximately 25 percent of the 90° fibers were observed to be longitudinally cracked after fatigue. The lamination theory would predict a loss of 15 percent in stiffness by eliminating the 90° fibers. Perhaps the split fibers account for some of the discrepancy between test and prediction. A 35 percent loss in stiffness was predicted to occur at $\Delta\epsilon = 0.004$, whereas the experimental results shown a 45 percent loss.

The predictions agree well with the data for the $[0/\pm 45/90]_S$ laminate as shown in Figure 10. This laminate is subject to a 40 percent loss in secant modulus when cycled at $\Delta\epsilon = 0.004$.

Behavior of $[\pm 45]_2S$ Laminate

The $[\pm 45]_2S$ laminate is unique among the laminates tested in that it has no 0° fibers to pick up the load from the damaged matrix as suggested in the previously discussed shakedown stiffness loss model. The 0° fibers also serve

to limit axial strain. Since the $[\pm 45]_{2s}$ laminate has no 0° fibers to limit axial deformation, large plastic deformations occurred in the specimen upon yielding. This can result in rotation of the $\pm 45^\circ$ fibers to approximately $\pm 39^\circ$.

The following is a description of observed behavior as a function of cyclic stress range:

Below the shakedown stress range (Fig. 11) of 150 MPa the specimen underwent large plastic deformation (as much as 0.08 strain). During cyclic loading, the matrix yield stress changed from its initial value of 40 MPa to a fully hardened, stabilized value of 150 MPa. The rotation of the fibers (to approximately $\pm 41^\circ$) actually causes the elastic modulus and secant modulus to increase slightly. The cross-sectional area of the specimen decreased by approximately 8 percent during a cyclic stress range of 138 MPa. The stress-strain behavior of the laminate stabilized. No fatigue damage was noticed.

Above the shakedown stress range, fatigue damage developed in the form of many matrix cracks growing into the specimen from the edge. Under these conditions the elastic modulus and the secant modulus of the laminate decrease. At $\Delta S = 172$ MPa the fibers rotated to $\pm 39^\circ$.

The exact values of the moduli were somewhat difficult to obtain because of the large scale plastic deformation and accompanying decrease in cross-sectional area. Figure 11 shows an S-N curve of the tests in terms of engineering stress (i.e., load/original area). The figure shows the predicted shakedown limit based on the original cross-sectional area and $\pm 45^\circ$ fiber orientation. The data indicate that the fatigue endurance limit at 2×10^6 cycles is approximately equal to the shakedown stress range. Once fatigue damage initiates in the matrix it will eventually grow to cause laminate

failure since there are no 0° fibers to pick up the load in a strain control fashion. Thus, the fatigue limit of laminates with no continuous 0° fibers may be predicted by the shakedown stress range. These type laminates do, however, undergo large plastic deformations below the shakedown down range, which may make them impractical for structural application at high stress levels. Perhaps some of this plasticity problem could be eliminated by heat-treating the matrix to a -T4 or -T6 condition.

SCS₂/Al versus B/Al Behavior

The stiffness loss of eight different lay-ups of B/Al composites were presented in reference [1]. Many of these lay-ups had the same fiber volume fraction and stacking sequence as the SCS₂/Al composites tested in the current work. The manufacturer's suggested fiber modulus for SCS₂ (390 GPa) is the same as the boron fiber (although, as previously discussed, we found the actual SCS₂ modulus to be closer to 340 GPa for the tested laminates). The SCS₂/Al has been suggested to be a more economical alternative to B/Al, therefore it is appropriate to directly compare the behavior of the two systems.

The B/Al showed superior fiber/matrix bonding. This was evident from less fiber pullout at failure surfaces (i.e., exposed matrix free fibers extending from the failure surface). Also, none of the previously tested B/Al laminates showed any signs of the delamination behavior illustrated in Figures 4-6.

Because the boron fiber modulus is higher than for SCS₂, the B/Al laminate's modulus is higher than the SCS₂/Al for equivalent fiber volume fraction and stacking sequence. The higher boron fiber modulus also results in a higher shakedown stress and higher stiffness above the shakedown stress. A typical example is shown in Figure 12 for the [0₂/±45]_S lay-up.

It is expected that the latest SCS₂ fibers [9] would result in laminates with comparable performance to B/Al.

The shakedown stiffness loss model predicts the behavior of SCS₂/Al as well as it did for B/Al in spite of the poor SCS₂ fiber/matrix bonds.

SUMMARY AND CONCLUSIONS

Four lay-ups of continuous fiber silicon carbide SCS₂ fiber/aluminum matrix composites were tested to assess stiffness loss when cycled below their respective fatigue limits. The lay-ups were [0]₈, [0₂/±45]_s, [0/90]_{2s}, and [0/±45/90]_s. The data were compared with predictions from the first author's previously published shakedown model which predicts fatigue-induced stiffness loss in metal matrix composites. A fifth lay-up, [±45]_{2s}, was tested to compare the shakedown and fatigue limits. The following observations were made:

- With the exception of the [±45]_{2s} laminate, the SCS₂/Al laminates exhibited significant stiffness loss when cycled below the fatigue limit. As an example, the quasi-isotropic laminate lost over 40 percent of the original stiffness.
- Most of the stiffness loss was attributed to fatigue cracks in the matrix material.
- The stiffness loss model predictions compared well with the data.
- The SCS₂ fibers were poorly bonded to the matrix in several laminates. This poor fiber/matrix bonding resulted in edge delaminations in one lay-up. ([0₂/±45]_s).
- The fatigue limit corresponds to the shakedown limit for the [±45]_{2s} laminate.
- The modulus of the SCS₂ fiber was found to be lower than reported by the manufacturer. The modulus was found to be approximately 340 GPa.

REFERENCES

- [1] Johnson, W. S., "Modeling Stiffness Loss in Boron/Aluminum Laminates Below the Fatigue Limit," *Long-Term Behavior of Composites*, ASTM STP 813, American Society of Testing and Materials, Philadelphia, 1983, pp. 160-176.
- [2] Johnson, W. S., "Mechanisms of Fatigue Damage in Boron/Aluminum Composites," *NASA TM-81926*, National Aeronautics and Space Administration, Washington, DC, Dec. 1980. (Also *Damage in Composite Materials*, ASTM STP 775, American Society for Testing and Materials, Philadelphia, pp. 83-102.)
- [3] Dvorak, G. J. and Johnson, W. S., "Fatigue of Metal Matrix Composites," *International Journal of Fracture*, Vol. 16, No. 6, Dec. 1980, pp. 585-607.
- [4] Johnson, W. S., "Characterization of Fatigue Damage Mechanisms in Continuous Fiber Reinforced Metal Matrix Composites," Ph.D. thesis, Duke University, Durham, NC, Dec. 1979.
- [5] Dvorak, G. J. and Johnson, W. S., "Fatigue Mechanisms in Metal Matrix Composite Laminates," *1981 Advances in Aerospace Structures and Materials*, ASME AD-01, American Society of Mechanical Engineers, New York, 1981, pp. 21-34.
- [6] Weng, M. T., "Some Aspects of Fatigue Relative to Cyclic Yield Stress," *International Journal of Fatigue*, Vol. 3, No. 3, Oct. 1981, pp. 187-193.
- [7] Bahei-El-Din, Y. A., "Plastic Analysis of Metal-Matrix Composite Laminates," Ph.D. thesis, Duke University, Durham, NC, July 1979.
- [8] Wawner, F. E., Teng, A. Y., and Nutt, S. R., "Microstructural Characterization of SiC(SCS) Filaments," *Metal Matrix, Carbon, and SiC Composites*, NASA Conference Publication 2291, November 1983.
- [9] Suplinskas, R. J., "Development of Low Cost Methods of Fiber Manufacture," 4th Monthly Technical Report, Sept. 24, 1984 (Submitted to AMMRC) Contract DAAG46-82-C-0033.

Table I. Composite Constituents Mechanical Properties

	SCS ₂ fiber 0.14 mm diameter	6061-T0 Aluminum
Elastic modulus, GPa	340	72.5
Poisson's ratio	0.25	0.33

TABLE II. Average SCS₂ Fiber Modulus, GPa

Gage length, mm	51	76	102
Lay-up			
[0] ₈	313	343	342
[0/90] _{2s}	307	332	----

Table III. Calculated and Experimental Elastic Moduli
and Calculated Shakedown Stress Range

Laminate	Experimental E_o , GPa	Calculated	
		E_o , GPa	ΔS_{sh} , MPa
$[0]_8$	191	190	368
$[0_2/\pm 45]_s$	158	154	199
$[0/90]_{2s}$	128	153	204
$[0/\pm 45/90]_s$	123	137	179
$[\pm 45]_{2s}$	101	118	150

FIGURES

Figure 1. - Matrix and fiber stress response to applied laminate stress prior to and after development of the saturation damage state.

Figure 2. - Composite laminate and matrix stress-strain response for a saturation damage state.

Figure 3. - Predicted versus experimental laminate elastic modulus.

Figure 4. - Edge view of fiber-matrix separation.

Figure 5. - Edge view of edge delamination due to weak fiber-matrix bonding.

Figure 6. - Radiograph of edge delamination

Figure 7. - Correlation of experimental and model prediction for $[0]_S$ laminates after 500,000 fatigue cycles.

Figure 8. - Correlation of experimental and model predictions for $[0_2/\pm 45]_S$ laminates after 500,000 fatigue cycles.

Figure 9. - Correlation of experimental and model predictions for $[0/90]_{2S}$ laminate after 500,000 fatigue cycles.

Figure 10. - Correlation of experimental and model predictions for $[0/\pm 45/90]_S$ laminate after 500,000 fatigue cycles.

Figure 11. S-N curve for $[\pm 45]_{2S}$ laminates.

Figure 12. Comparison of B/Al and SCS₂/Al composite stiffness loss behavior after 500,000 load cycles.

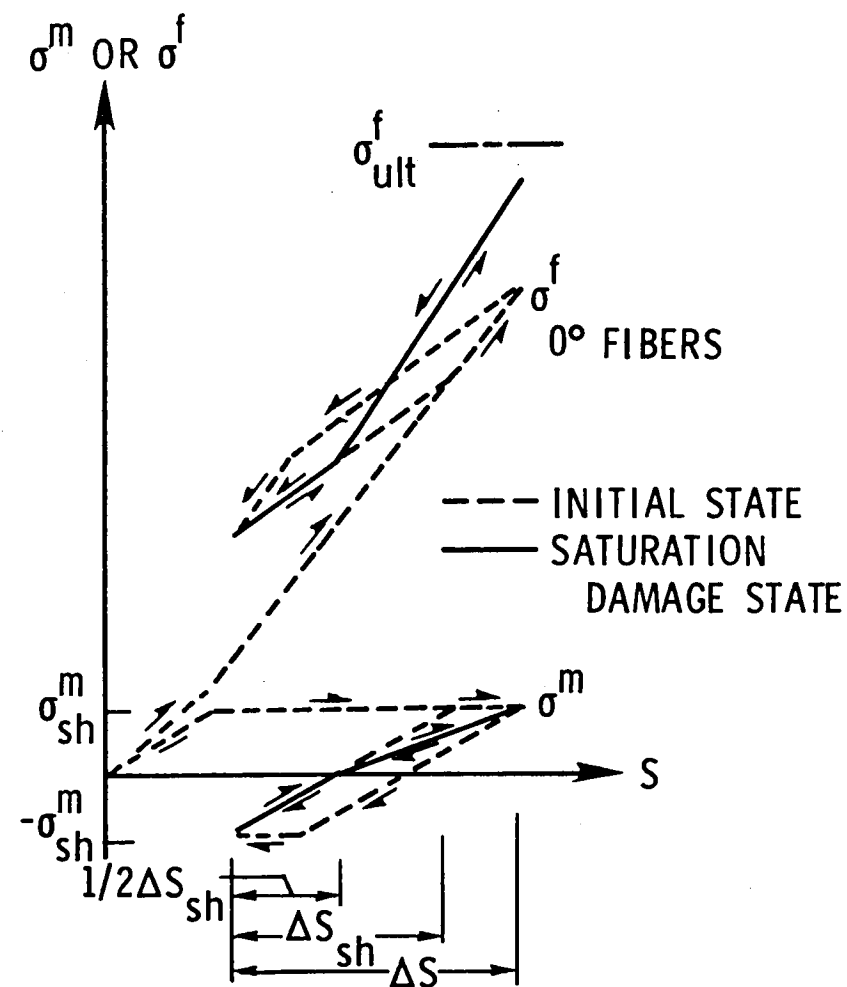


Figure 1. - Matrix and fiber stress response to applied laminate stress prior to and after development of the saturation damage state.

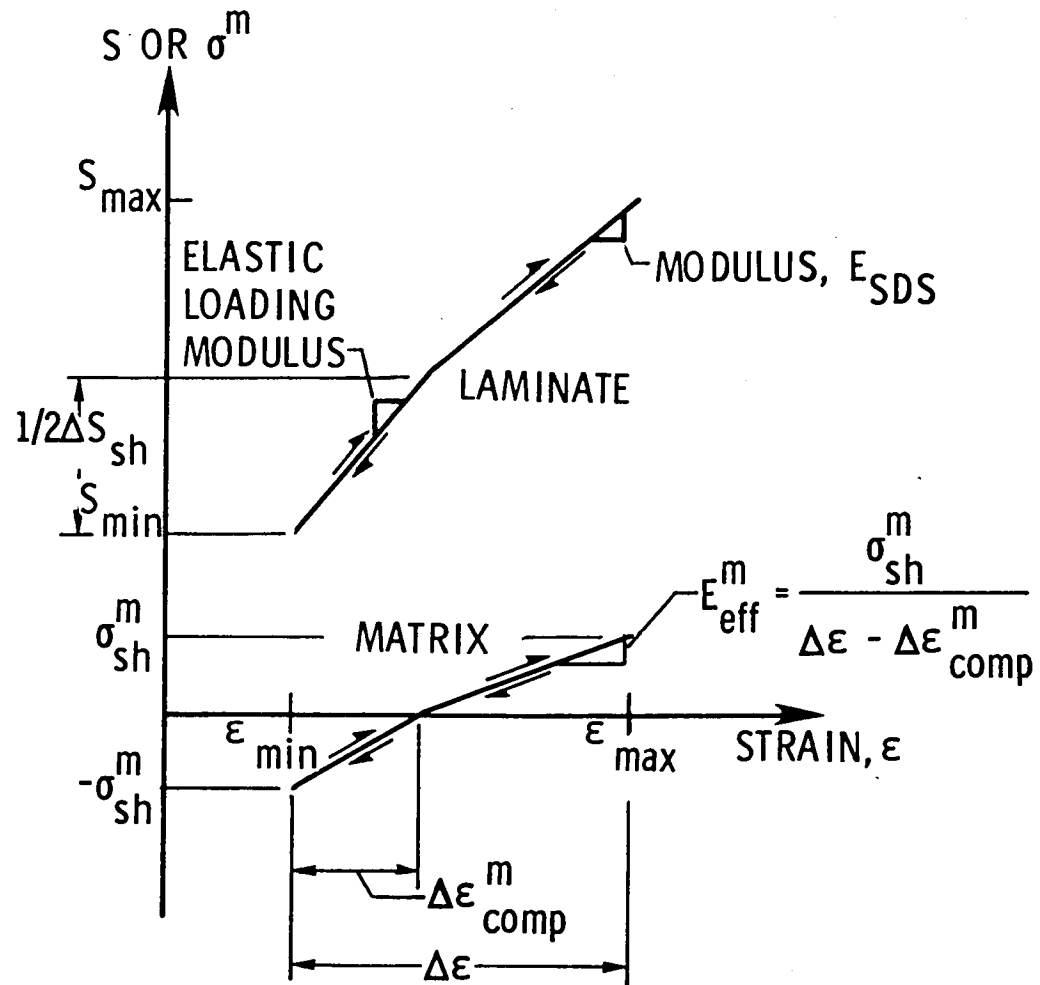


Figure 2. - Composite laminate and matrix stress-strain response for a saturation damage state.

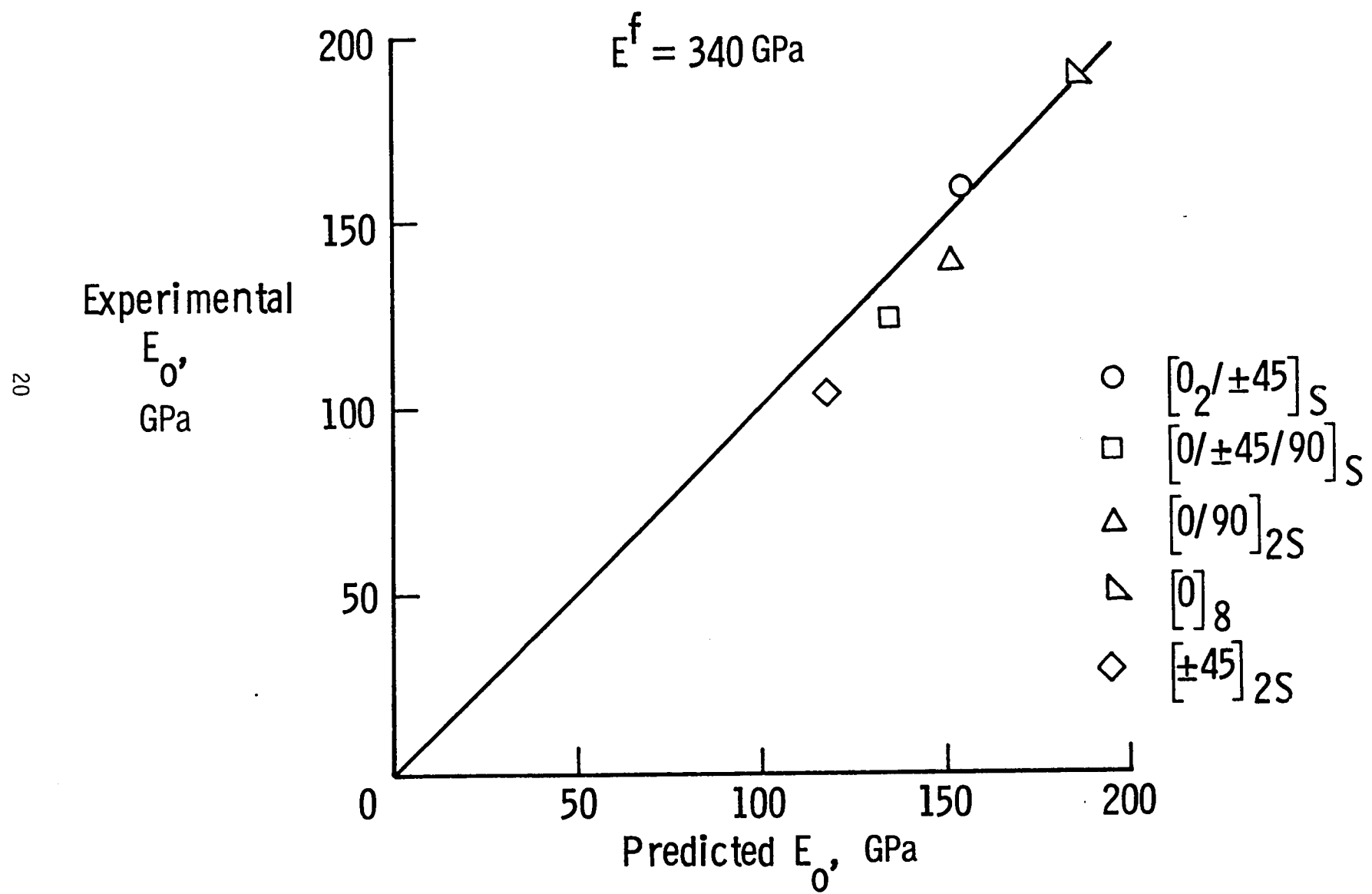


Figure 3. - Predicted versus experimental laminate elastic modulus.

SCS₂/AL
 $[0_2/\pm 45]_S$
 $\Delta S = 455$ MPa
500k Cycles

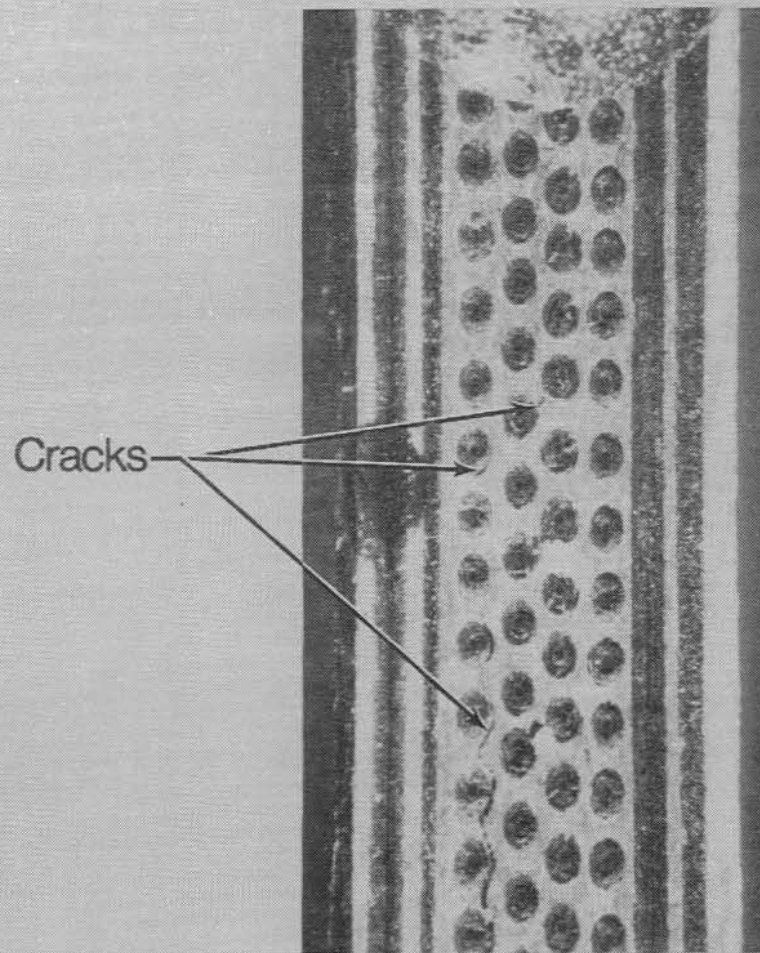


Figure 4. - Edge view of fiber-matrix separation.

SCS₂/AL
[0₂/±45]_S
ΔS = 525 MPa
1000k Cycles

Edge
Delamination

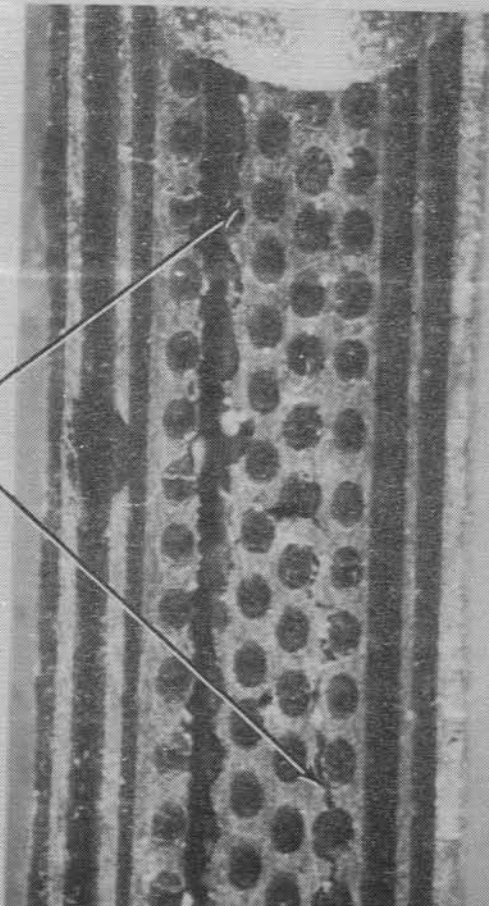


Figure 5. - Edge view of edge delamination due to weak fiber-matrix bonding.

SCS₂/AL
 $[0_2/\pm 45]_S$
 $\Delta S = 560$ MPa
1500k Cycles

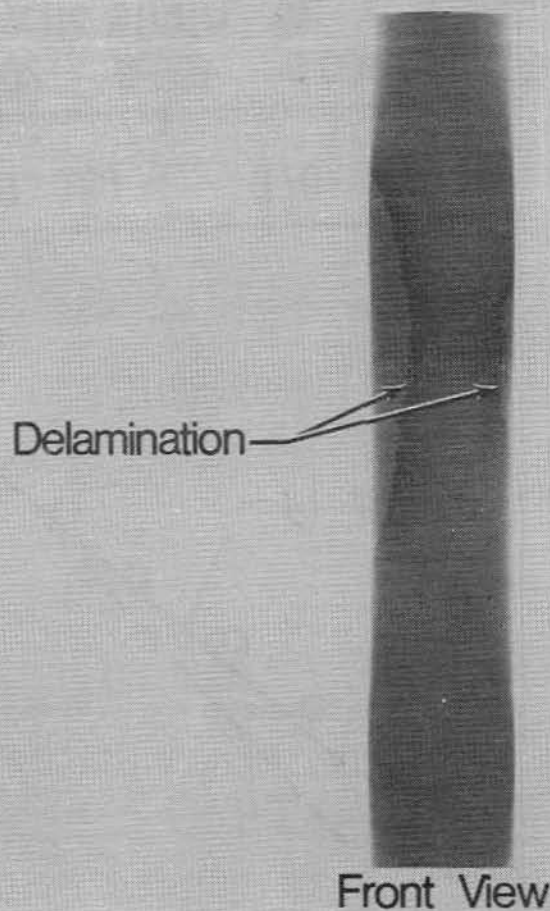


Figure 6. - Radiograph of edge delamination

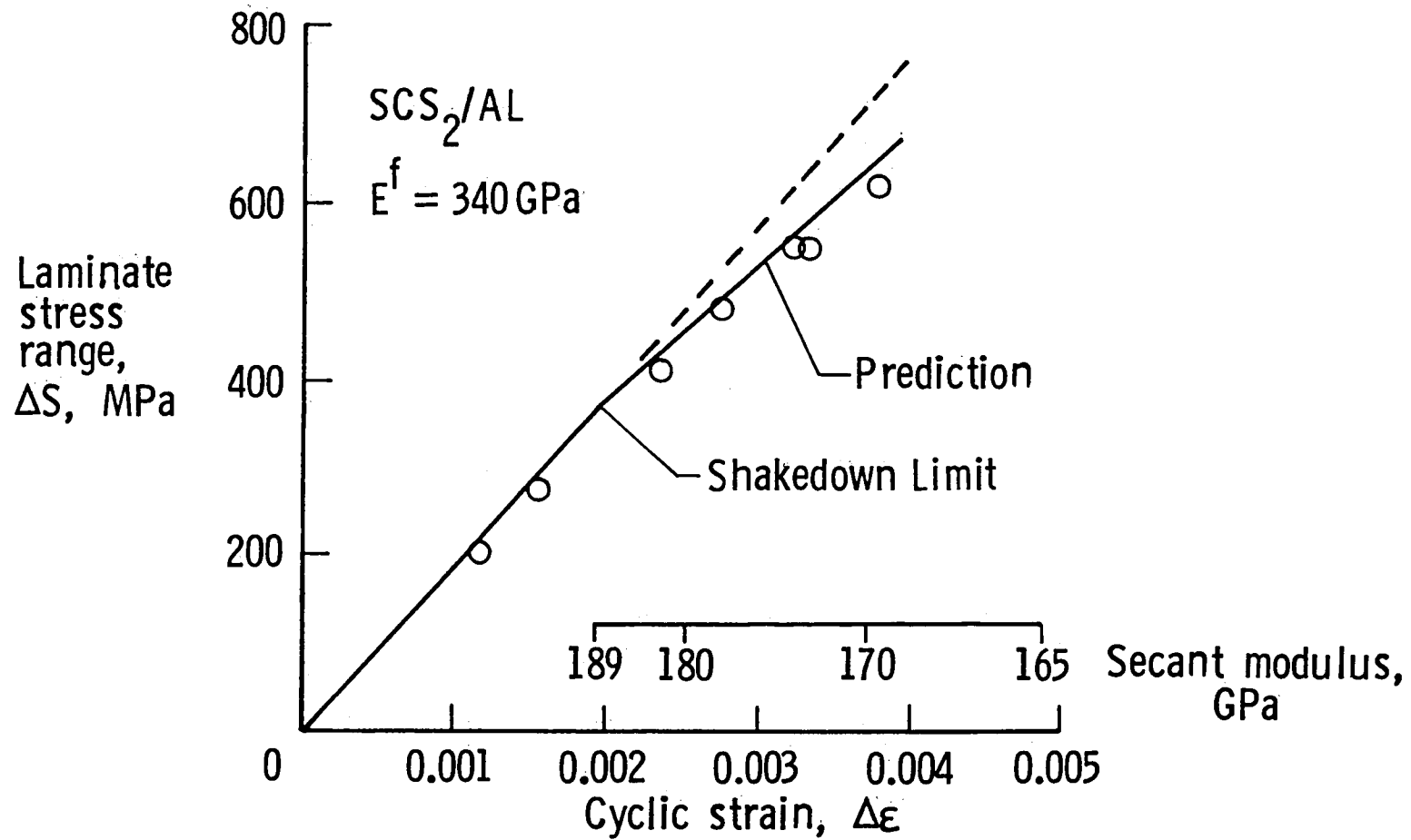


Figure 7. - Correlation of experimental and model prediction for $[0]_s$ laminates after 500,000 fatigue cycles.

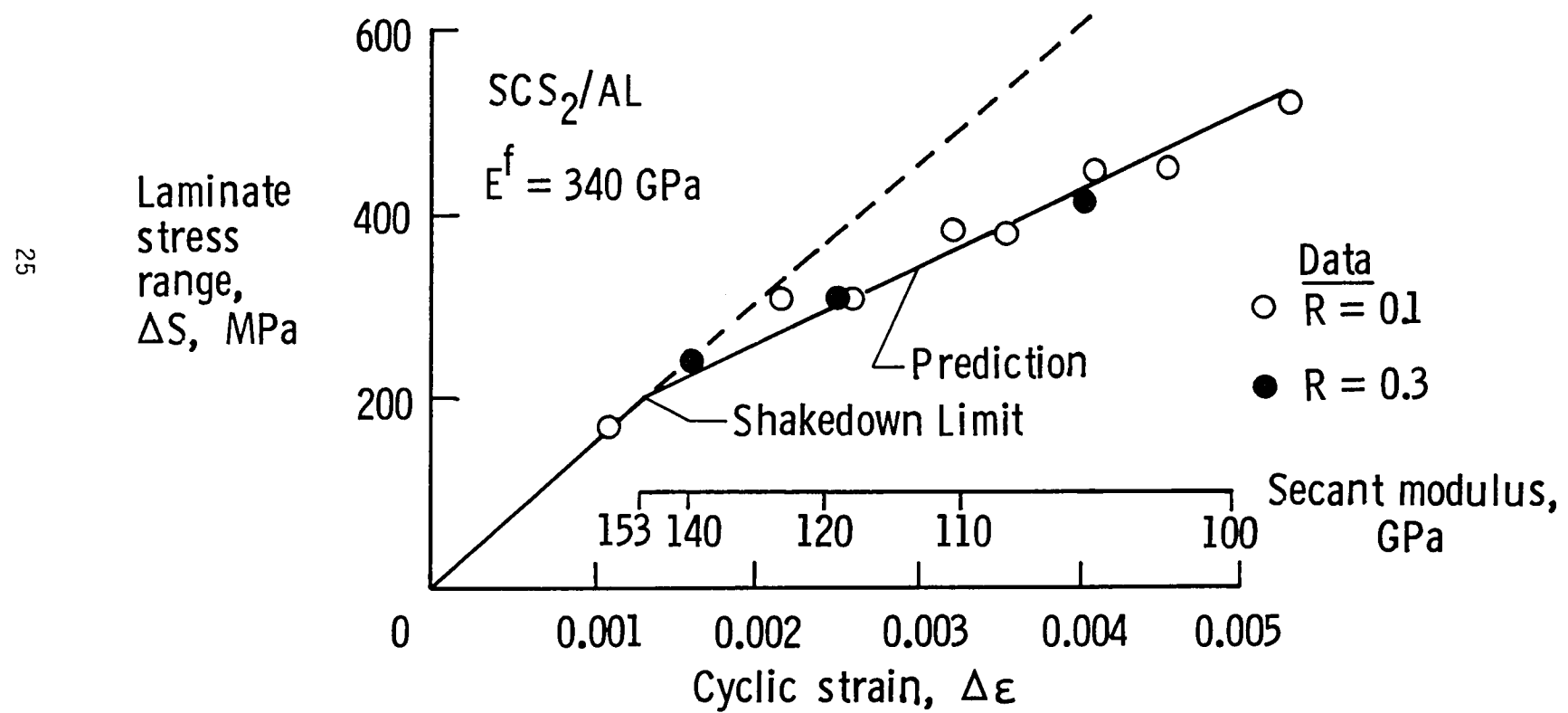


Figure 8. - Correlation of experimental and model predictions for $[0_2/\pm 45]_S$ laminates after 500,000 fatigue cycles.

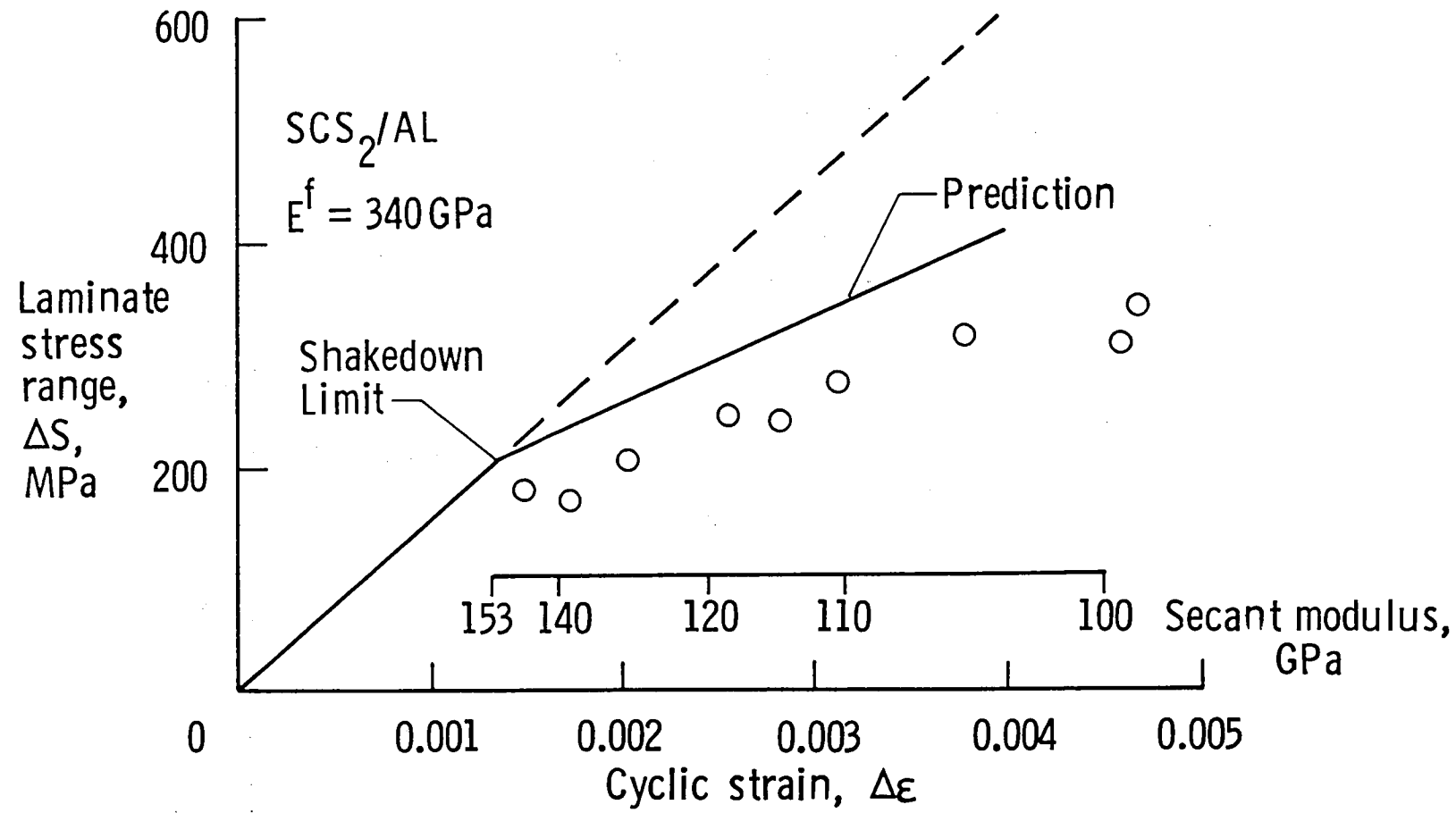


Figure 9. - Correlation of experimental and model predictions for $[0/90]_{2s}$ laminate after 500,000 fatigue cycles.

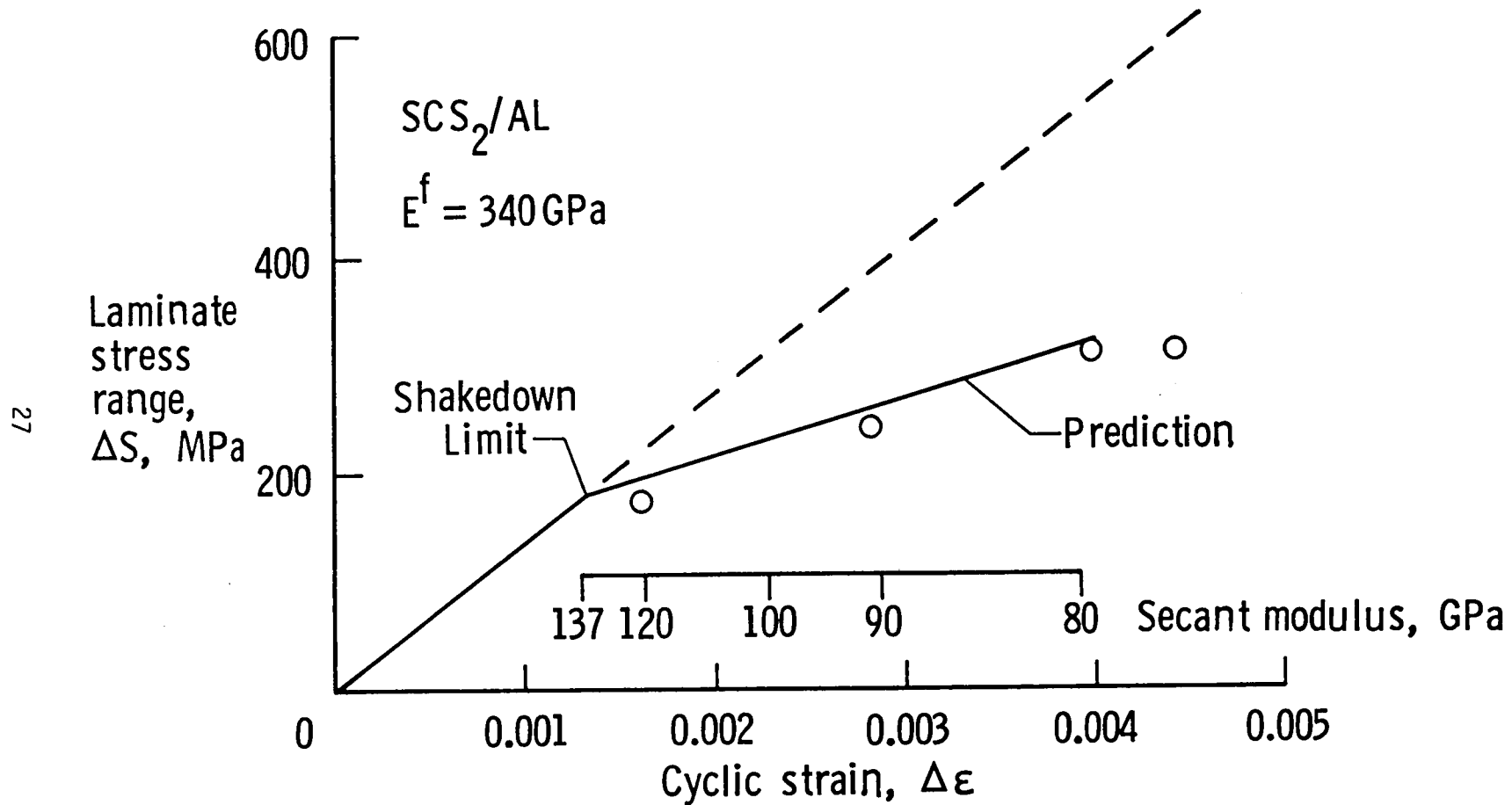


Figure 10. - Correlation of experimental and model predictions for [0/±45/90]_s laminate after 500,000 fatigue cycles.

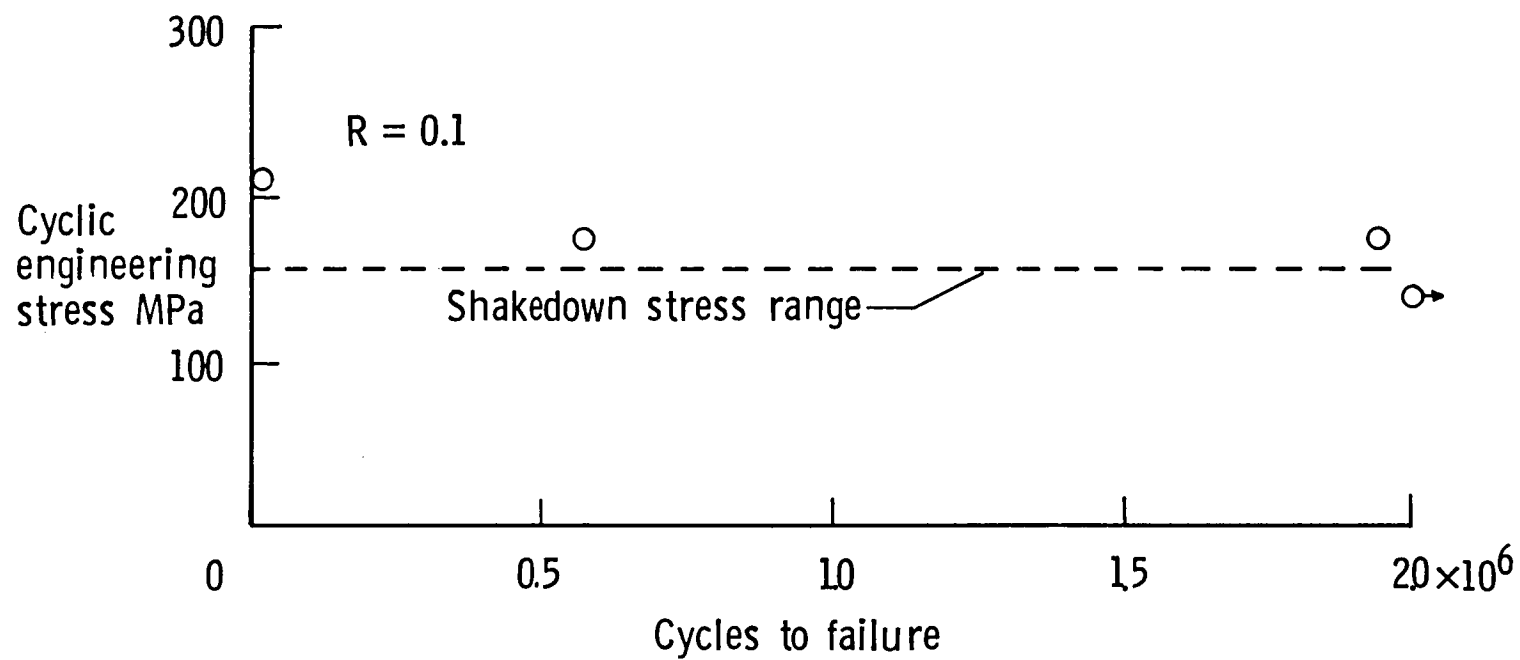


Figure 11. S-N curve for $[\pm 45]_{2s}$ laminates.

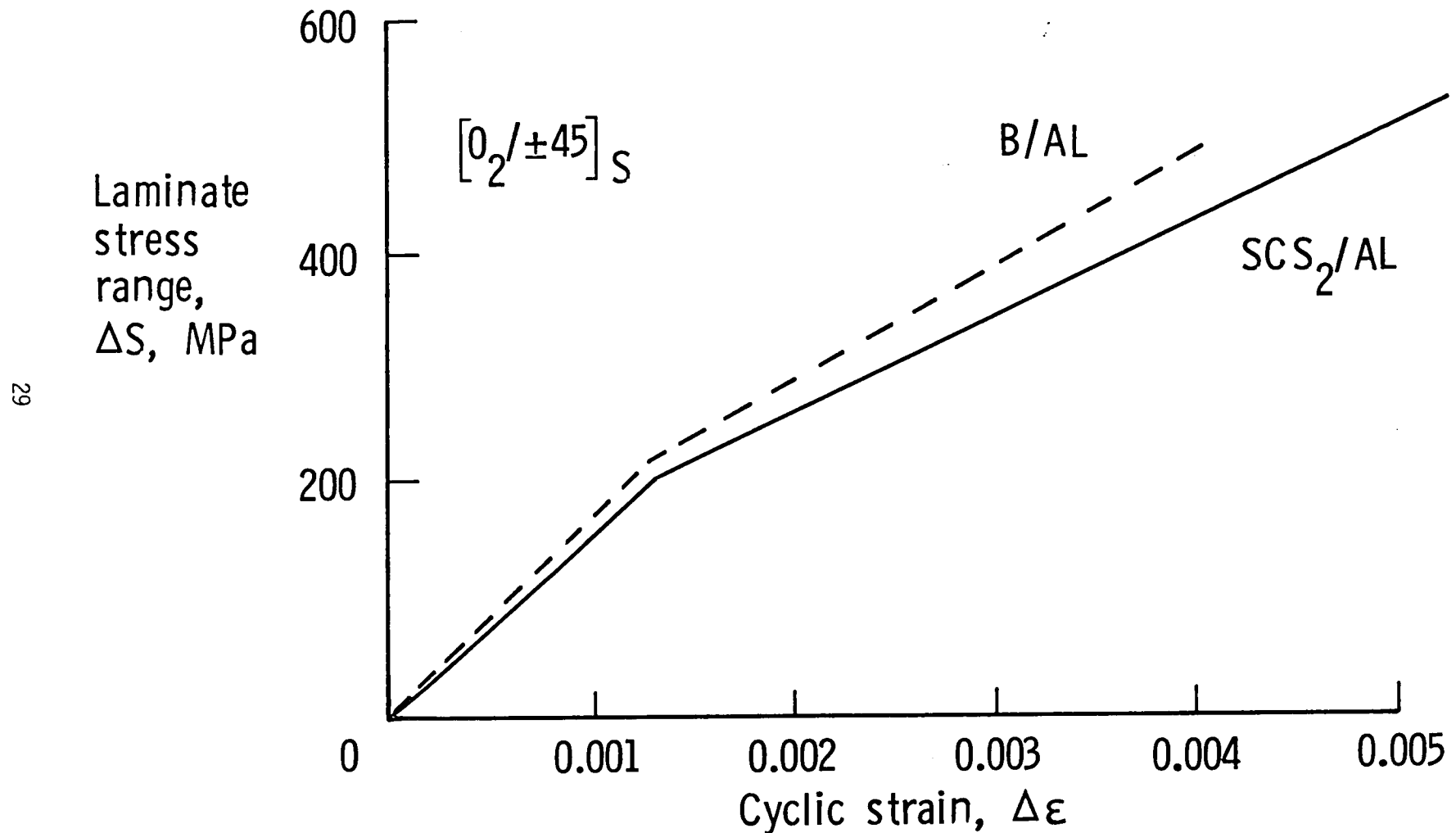


Figure 12. Comparison of B/Al and SCS₂/Al composite stiffness loss behavior after 500,000 load cycles.

1. Report No. NASA TM-86332	2. Government Accession No.	3. Recipient's Catalog No.	
4. Title and Subtitle Fatigue Behavior of Continuous Fiber Silicon-Carbide/Aluminum Composites		5. Report Date December 1984	6. Performing Organization Code 505-33-33-05
7. Author(s) W. S. Johnson *R. R. Wallis		8. Performing Organization Report No.	
9. Performing Organization Name and Address NASA Langley Research Center Hampton, VA 23665		10. Work Unit No.	
12. Sponsoring Agency Name and Address National Aeronautics and Space Administration Washington, DC 20546		11. Contract or Grant No.	
15. Supplementary Notes *R. R. Wallis, Co-op student, Virginia Polytechnic Institute and State University.		13. Type of Report and Period Covered Technical Memorandum	
14. Sponsoring Agency Code			
16. Abstract Four lay-ups of continuous fiber silicon carbide (SCS_2) fiber/aluminum matrix composites were tested to assess fatigue mechanisms including stiffness loss when cycled below their respective fatigue limits. The lay-ups were $[0]_8$, $[0_2/\pm 45]_{2s}$, $[0/90]_{2s}$, and $[0/\pm 45/90]_s$. The data were compared with predictions from the author's previously published shakedown model which predicts fatigue-induced stiffness loss in metal matrix composites. A fifth lay-up, $[\pm 45]_{2s}$, was tested to compare shakedown and fatigue limits. The particular batch of silicon-carbide fibers tested in this program had a somewhat lower modulus (340 GPa) than expected and displayed poor bonding to the aluminum matrix. Good agreement was obtained between the stiffness loss model and the test data. The fatigue damage below the fatigue limit was primarily in the form of matrix cracking. The fatigue limit corresponded to the laminate shakedown for the $[\pm 45]_{2s}$ laminate.			
17. Key Words (Suggested by Author(s)) fatigue, metal matrix composites, stiffness loss, silicon carbide fibers, aluminum matrix		18. Distribution Statement Unclassified - Unlimited Subject Category - 24	
19. Security Classif. (of this report) Unclassified	20. Security Classif. (of this page) Unclassified	21. No. of Pages 30	22. Price A03

